Title
Influence of dislocations and twin walls in BaTiO3 on the voltage-controlled switching of perpendicular magnetization

Journal
Physical Review Materials, 5(2)

ISSN
2476-0455

Authors
Goiriena-Goikoetxea, M
Xiao, Z
El-Ghazaly, A
et al.

Publication Date
2021-02-01

DOI
10.1103/physrevmaterials.5.024401

Peer reviewed

Influence of dislocations and twin walls in $BaTiO_3$ on the voltage-controlled switching of perpendicular magnetization

M. Goiriena-Goikoetxea[1,2,*], Z. Xiao[3,4], A. El-Ghazaly[1], C. V. Stan[4,5], J. Chatterjee[1], A. Ceballos[6,7], A. Pattabi[1], N. Tamura[4], R. Lo Conte[1], F. Hellman[6,7,8], R. Candler[3,9] and J. Bokor[1,7]

[1]*Department of Electrical Engineering and Computer Sciences, University of California, Berkeley, California 94720, USA*

[2]*Department of Electricity and Electronics, University of the Basque Country, Leioa 48940, Spain*

[3]*Department of Electrical and Computer Engineering, University of California, Los Angeles, California 90095, USA*

[4]*Advanced Light Source, Lawrence Berkeley National Lab, Berkeley, California 94720, USA*

[5]*NIF and Photon Science, Lawrence Livermore National Laboratory, Livermore, California 94551, USA*

[6]*Department of Materials Science and Engineering, University of California, Berkeley, California 94720, USA*

[7]*Materials Science Division, Lawrence Berkeley National Laboratory, Berkeley, California 94720, USA*

[8]*Department of Physics, University of California, Berkeley, California 94720, USA*

[9]*California NanoSystems Institute, Los Angeles, California 90095, USA*

We investigate the influence of dislocations and twin walls in $BaTiO_3$ on its ferroelectric response and the resulting effect on the perpendicular magnetic anisotropy (PMA) of a strain-coupled $[Co\backslash Ni]_n$ film. A dense twinned structure in conjunction with a high dislocation density significantly reduces the converse piezoelectric effect of $BaTiO_3$ by hindering the propagation of newly nucleated domains with an applied electric field. This, in turn, results in a modest reduction of the PMA of the ferromagnetic layer. On the other hand, the ferroelectric polarization reorients from [100] to [001] direction in a dislocation-free $BaTiO_3$, inducing the maximum achievable in-plane compressive strain of 1.1%. A large fraction of this uniaxial strain is transferred to the magnetoelastically coupled ferromagnetic layers whose magnetization switches to in-plane via the inverse magnetostriction effect. This work reveals the critical role of the interplay between twin walls and dislocations within a ferroelectric substrate in the performance of multiferroic heterostructures and provides insight into the development of highly energy-efficient magnetoelectric devices.

Controlling magnetization at small scales with electric fields opens up new prospects for highly energy-efficient logic [1,2] and memory devices [3]. Conventionally, magnetization has been electrically controlled via spin-transfer torque [4] and, more recently, by spin-orbit torque [5]. However, both mechanisms use electric currents resulting in significant Ohmic heating losses, leading to low energy efficiency. Voltage control of magnetism arises as a promising alternative to power-consuming current-based approaches. One voltage-controlled system is based on strain-mediated multiferroic heterostructures, where a ferromagnetic

[*]maite.goiriena@ehu.eus

layer and a ferroelectric substrate are coupled together magnetoelastically [6]. In this system, the application of an electric field induces lattice strains in the ferroelectric substrate (via the converse piezoelectric effect), which are transferred to the ferromagnetic layer, resulting in the alteration of its magnetocrystalline anisotropy. In particular, multiferroic heterostructures based on the ferroelectric $BaTiO_3$ have proven to be a notably effective magnetoelectric system [7-12].

In a $BaTiO_3$ crystal, which exhibits a tetragonal cell structure at room temperature (a = 3.992 Å, c = 4.036 Å), two types of ferroelectric domains may coexist: *a*-domains with in-plane ferroelectric polarization and *c*-domains with out-of-plane polarization. The in-plane lattice structure in the *a*-domains is rectangular, whereas in the *c*-domains is square, as shown in the schematic illustrations in Fig. 1(a). In the case of an initial in-plane polarization (*a*-domains), application of an out-of-plane electric field shifts the body-centered Ti atom along the direction of the field. This shift gives rise to a lattice distortion, which can be visualized as a switching from *a*-domains to *c*-domains and is accompanied by an in-plane compressive strain of 1.1%.

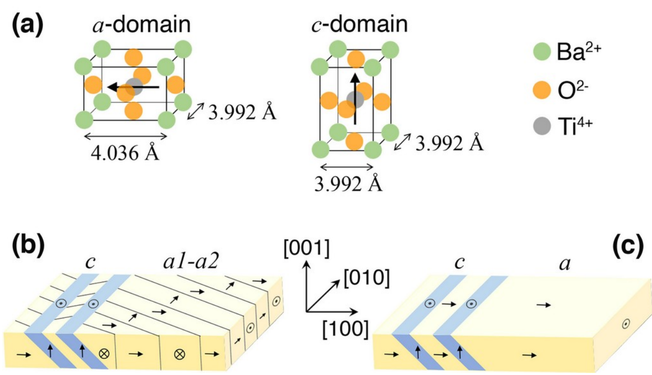

FIG. 1. (a) Orientation of the $BaTiO_3$ tetragonal cell in the ferroelectric *a*- and *c*-domains; the black arrows indicate the direction of the ferroelectric polarization. (b, c) Schematic illustrations of the ferroelectric domain configuration in BTO-1 (b), which is characterized by a dense *a1-a2* twinning and random *c*-domains, and in BTO-2 (c), with a predominantly *a*-domain configuration alternated with random *c*-domains.

Besides the intrinsic contribution of the unit cell distortion caused by an applied electric field, the converse piezoelectric effect of a ferroelectric material is also affected by extrinsic contributions that are mainly due to the motion of non-180° ferroelectric domain walls [13,14]. In $BaTiO_3$, 90° domain walls correspond to {101} twin planes and can be subdivided into *a-c* and *a1-a2* walls [15]. These twin walls are two-dimensional lattice defects, with different electronic and structural symmetry from their parent material, and act as nucleation sites that determine the polarization dynamics in the absence of other defects [16]. Nonetheless, defects such as oxygen vacancies, point charges and dislocations play a crucial role in the

*maite.goiriena@ehu.eus

polarization switching since they interact with twin walls at the atomic scale. Among these defects, dislocations (one-dimensional defects) are of particular relevance for they have been observed to impose a potential barrier on the twin wall, limiting its translational mobility under an applied electric field [17]. Hence, macroscopic ferroelectric switching is largely governed by defects and understanding their interaction is key to controlling it.

The interplay between dislocations and twin walls in $BaTiO_3$ was first observed by R. C. Bradt *et al.* who reported on dislocations serving as twin domains nucleating sites and then preventing the motion of twin walls by pinning them through strain interaction [18]. More recently, A. Kontsos *et al.* provided a theoretical framework to investigate the interactions between twin walls and dislocations in single crystal $BaTiO_3$ [19]. Their results showed that the interaction between twin walls and dislocations is affected by externally applied electric fields, which force the walls to move while this motion is hindered by the dislocations. Here, we present an experimental study of the influence of the coexistence of dislocations and twin walls in single crystal $BaTiO_3$ on its ferroelectric switching. The study is carried out by investigating two models of $BaTiO_3$ single crystals (described below) under a uniformly and systematically applied external electric field, in contrast to the simulated field conditions used in Ref. [18]. Furthermore, we extend the study to the subsequent effect on the voltage-controlled switching of a strain-coupled ferromagnetic element, namely $[Co\backslash Ni]_n$ multilayers with PMA. In this regard, we are unaware of any studies directly correlating dislocations and twin walls in the ferroelectric substrate with the degree of electric-field-controlled switching of the magnetic element, in the context of a multiferroic heterostructure. Concomitantly, the potential of the $BaTiO_3\backslash[Co\backslash Ni]_n$ system is assessed based on the applicability of electrical modulation of PMA in high-density magnetic data storage devices [20,21].

In the experiments, we investigate two types of single crystal $BaTiO_3$ (100) substrates, one serving as the model with dense arrays of twin domains and dislocations (hereafter called BTO-1) and the other one serving as an ideally defect-free $BaTiO_3$ (hereafter called BTO-2) (see section A in Supplemental Material for more information regarding the substrates [22]). These features were characterized by the Laue diffraction patterns, acquired from the X-ray microdiffraction (beamline 12.3.2, Advanced Light Source, Lawrence Berkeley National Laboratory)[23] using an X-ray wavelength range of 0.5-2 A and a beam size of 1.5 μm. The indexing of the Laue patterns allows determining important features of the crystals such as the orientations of each twin domain, and thus, how these orientations relate to each other, *i.e.* what are the twin planes and the twin domains (*a1, a2* or *c*). The acquired Laue diffraction patterns are shown in Fig. 2. As observed in the zoomed-in image on the top right of Fig. 2(a), BTO-1 exhibits twin domains corresponding to *a1-a2* domains but also *c*-domains, to a much lower extent. The corresponding twin walls all belong to the {101} family of planes. A schematic illustration of the

[*]maite.goiriena@ehu.eus

ferroelectric domain configuration in BTO-1 in the initial state is provided in Fig. 1(b). More importantly, the peaks are non-Gaussian, showing a large asymmetric broadening, which indicates the presence of dislocations. Indeed, white beam (*i.e.* Laue) X-ray diffraction measures local curvature of the lattice; if the local curvature is large, as in the case of BTO-1, dislocations have to be introduced to account for it [24]. Dislocations are classified into geometrically necessary dislocations (GNDs) and statistically stored dislocations (SSDs) [25,26]. GNDs represent the excess dislocations stored within a Burger's circuit and contribute to lattice curvature. Therefore, its density can be calculated from the local curvature measured by Laue diffraction data as $\rho = w/bL$ (where w is the full-width half-maximum corresponding to the larger lateral size of the c peak $(1\acute{1}5)$, $w = 0.243°$, b is the magnitude of the Burgers vector for $BaTiO_3$, $b = a[110]/2 =$¿ 0.28 nm, and L is the beam size, $L =$¿1.5 μm). The resulting value is 10.1×10^{10} cm^{-2}, a value well above what is considered a low dislocation density in $BaTiO_3$ [27]. In contrast, SSDs result in no curvature of the crystal lattices at length scales larger than the Burger's circuit being considered and consist of dipoles, multiples and loops within the Burger's circuit [28]. In any case, statistically stored dislocations are present in addition to geometrically necessary dislocations, thus the calculated density for BTO-1 sample is actually a lower bound.

On the other hand, the diffraction pattern of BTO-2 (Fig. 2(b)) corresponds to a single ferroelectric *a*-domain, with a well-defined Gaussian peak for each reflection, which indicates that the presence of dislocations in BTO-2 is negligible. It should be noted that the diffraction patterns are taken within a scanning area of 200×200 μm^2 which does not cover the entire $BaTiO_3$ crystal surface. Thus, polarized light microscopy was used as a complementary technique to characterize the ferroelectric domain configuration in BTO-1 and BTO-2 (see section B in Supplemental Material [22]). In fact, the microscopy images reveal the existence of random *c*-domains in BTO-2 that are not present in the X-ray scanned area. A schematic illustration of ferroelectric domain configuration in BTO-2 in the initial state is shown in Fig. 1(c).

*maite.goiriena@ehu.eus

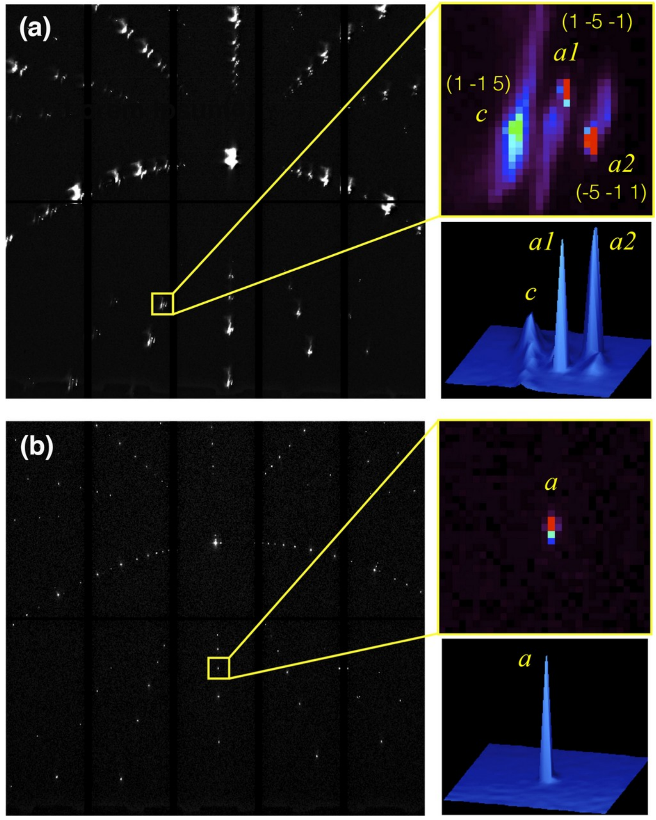

FIG. 2. Laue diffraction patterns of (a) BTO-1 and (b) BTO-2. The peaks marked in yellow frames are zoomed in on the top right and 3D surface plotted on the bottom right.

X-ray microdiffraction also provides mapping of crystallographic properties during *in-operando* conditions (application of voltage) with micrometer-scale resolution. Each pixel-point on the resulting map originates from an individual diffraction pattern that yields information about lattice strain and crystal orientation at the specific spatial location (pixel) of the 2D *x*-*y* plane. Therefore, it is an excellent technique to study the converse piezoelectric effect of our $BaTiO_3$ crystals at the microscale [23]. In order to apply voltage through the $BaTiO_3$ thickness, *i.e.* along the [001] direction, 50 nm Pt electrodes were evaporated onto both the top and the bottom surface of BTO-1 and BTO-2. The maps in Fig. 3 represent the orientation of the polar axis of the $BaTiO_3$ tetragonal cell with respect to the sample surface normal (*i.e.* the [001] direction), where an angle of 90° is equivalent to *a*-domains and one of 0° is equivalent to *c*-domains (see schematic descriptions in Fig. 3(e) and (f)).

In BTO-1, *a1*-, *a2*- and *c*-domains coexist in the initial state as shown in Fig. 3(a) (*a1* and *a2* stripe-domains can be distinguished by slightly different shades of yellow). This ferroelectric configuration remains almost unchanged during the application of an electric field up to 0.7 MV m^{-1} (Fig. 3(b)). It is noteworthy that a nucleation and a finite expansion of a small *c*-domain (see red frame in Fig. 3(b)) is observed, as well as the shrinkage of the initial stripe-like *c*-domain along the

*maite.goiriena@ehu.eus

center. The latter can be explained by the direction of the electric field being antiparallel to that of the ferroelectric polarization of the initial *c*-domain [29]. Other minor microscopic changes can be also distinguished (see section C in Supplemental Material [22] for a more detailed analysis). However, the overall response is insignificant even under an electric field of 0.7 MV m^{-1}, which is around seven times larger than the coercive field of $BaTiO_3$ [30]. This behavior could be attributed to large accumulations of dislocation that prevent the motion of twin walls by pinning them through strain interaction, resulting in the disruption of the propagation of newly nucleated *c*-domains. Indeed, when a twin wall is directly linked to a dislocation, the strain fields of the two might partially cancel out, resulting in lower energy. Thus, the twin wall is likely to be pinned at the dislocation site. Moreover, it has been recently reported that the application of an electric field to $BaTiO_3$ induces intense lattice distortion at the intersection region of twin domains, forming new dislocations [31].

On the contrary, BTO-2 starts with an in-plane ferroelectric configuration (in the scanned area of 200 × 200 μm^2) and switches to an out-of-plane orientation at only 0.08 MV m^{-1}. In this case, since BTO-2 has a dislocation-free microstructure, the initially present *c*-domains (shown in the polarized light microscopy image, Supplemental Material [22] section B) expand at the expense of *a*-domains in an undisrupted manner upon application of the electric field.

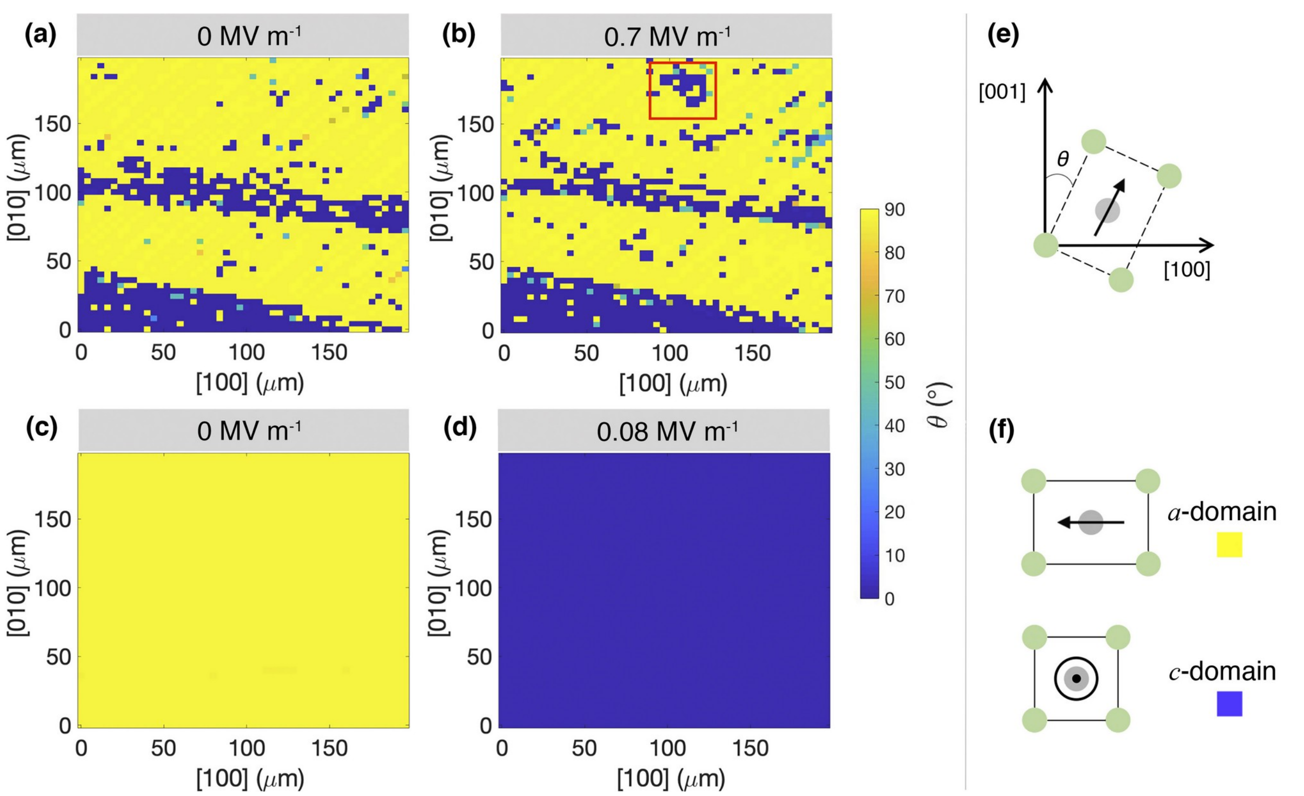

FIG. 3. $BaTiO_3$ tetragonal cell orientation with respect to the direction normal to the sample surface (*i.e.* [001] direction), before and after applying an electric field along the [001] direction of BTO-1 (a, b) and BTO-2 (c, d). The red frame in (b) indicates a small *c*-domain nucleated at 0.7 MV m^{-1}. (e) An angle of 90° is equivalent to *a*-domains and 0° is equivalent to *c*-domains. (f) In-plane lattice structure in *a*-domains (yellow) and *c*-domains (blue). The oxygen atoms have been removed from the scheme for simplicity.

*maite.goiriena@ehu.eus

In BTO-1, the in-plane strain is only induced in those areas where small *c*-domains were nucleated to replace the initial *a*-domains and in the areas where we observe a motion of pre-existing ferroelectric domain walls (*a**c* walls). However, in BTO-2, the strain is homogeneous with a mean value of -1.110 ± 0.008% (see section D in Supplemental Material [22] for more details) which is in agreement with the theoretical strain value reported in the literature [10]. From this result, we can estimate the maximum magnetoelastic anisotropy that can be electrically induced in the [Co\Ni]$_n$ multilayer investigated in our experiments (*i.e.* 4 bilayers of 0.15 nm thick Co and 0.6 nm thick Ni, topped with an additional 0.15 nm thick Co layer, for symmetry, hereafter called [Co\Ni]$_4$) as $K_{me}=\frac{-3}{2}\lambda_s \varepsilon Y$ [32]. λ_s and *Y* are respectively the saturation magnetostriction and Young's modulus of the [Co\Ni]$_4$ stack ($\lambda_s=\frac{2.4\,\lambda_s^{¿}+0.75\,\lambda_s^{Co}}{3.15}$, $Y=\frac{2.4\,Y_{¿}+0.75\,Y_{Co}}{3.15}$; where $\lambda_s^{¿}=-35\,ppm$, $\lambda_s^{Co}=-60\,ppm$, $Y_{¿}=200\,GPa$, $Y_{Co}=209\,GPa$) [33,34], and $\varepsilon=-¿1.1\%$ is the measured strain in the BTO-2 substrate. Based on these material parameters, the electrically induced magnetoelastic anisotropy in BTO-2\[Co\Ni]$_4$ is expected to be $K_{me}=-¿136$ kJ cm^{-3}, which is larger than the PMA energy measured in an identical [Co\Ni]$_4$ multilayer [35], anticipating that the magnitude of electrically induced strains in BTO-2 is sufficient to switch the magnetization from out-of-plane to in-plane.

For the study of electric field driven manipulation of magnetization, [Co\Ni]$_4$ multilayers with PMA were deposited by DC magnetron sputtering on the $BaTiO_3$ substrates. The same stack was deposited on BTO-1 and BTO-2 consisting in Ta(1)\Pt(3)\[Co(0.15)\Ni(0.6)]$_4$\Co(0.15)\Pt(3), with the top Pt and a continuous metallic thin film on the backside of the crystals serving as the top and the bottom electrodes. Magneto-optic Kerr effect (MOKE) microscopy with polar geometry was used to measure the out-of-plane hysteresis curves, *i.e.* the applied magnetic field is normal to the surface of the sample. The electric field was applied along the [001] direction from 0 MV m^{-1} to 0.8 MV m^{-1}, with a step size of 0.08 MV m^{-1}, taking a hysteresis loop at each step. Fig. 4(a) and (b) display the magnetic loops corresponding to the electric field steps at which the change in the magnetization was first observed for BTO-1\[Co\Ni]$_4$ and BTO-2\[Co\Ni]$_4$, respectively.

In BTO-1\[Co\Ni]$_4$ sample, it is not until the electric field step of 0.8 MV m^{-1} that we observe a variation in the magnetization, which is characterized by a lower magnetic coercivity and a less abrupt magnetization reversal process (the

*maite.goiriena@ehu.eus

“squareness” of the loop, calculated as the ratio of remanent to saturation magnetization, M_R/M_S, decreases from 0.97 to 0.87). These features indicate that the PMA has been reduced, as observed in other ferroelectric\PMA heterostructures [35,36]. The dependence of the out-of-plane coercive field of $[Co\backslash Ni]_4$ on the applied electric fields is shown in the inset of Fig. 4(a). Since the magnetostrictive coefficients of polycrystalline Co and Ni thin films have negative signs, the magnetization will tend to align with the compressive strain. Therefore, the compressive strain induced in the plane of BTO-1 and transferred to the $[Co\backslash Ni]_4$ multilayer would reduce its PMA, leading to smaller out-of-plane coercive fields, which is consistent with the shape of the butterfly-like E-$H_{\perp c}$ loop in the inset. However, the PMA reduction is small as a consequence of the low degree of ferroelectric domain reorientation shown in Fig. 3(a) and 3(b). Another observation on the E-$H_{\perp c}$ loop is that the $H_{\perp c}$ at 0 MV m^{-1}, after positive and negative poling, decreases compared to the initial value, which may be a sign of ferroelectric fatigue caused by an increase of defect density. As mentioned earlier, the application of an electric field to $BaTiO_3$ induces lattice distortion at the intersection of twin domains and forms new dislocations [31]. Consequently, twin wall pinning events would also increase, hindering BTO-1 from relaxing into *a*-domains upon removal of the electric field, and reducing both the ferroelectric and the magnetic switching reversibility in this particular system.

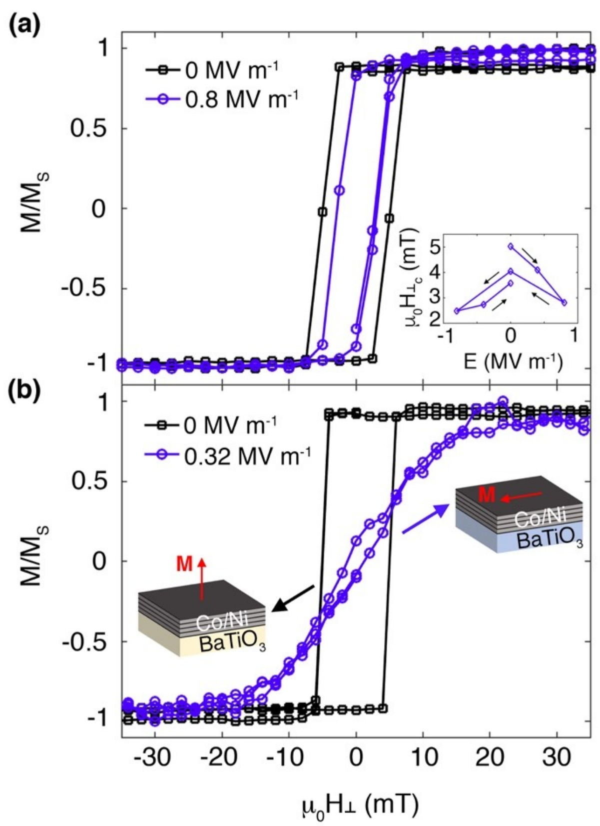

[*]maite.goiriena@ehu.eus

FIG. 4. Modulation of the out-of-plane magnetization in $[Co\backslash Ni]_4$ multilayers controlled by a voltage applied along the [001] direction of BTO-1 (a) and BTO-2 (b). The inset in (a) shows the dependence of the out-of-plane coercive field on the electric field, which was varied in the order indicated by the arrows.

On the other hand, BTO-2 is capable of inducing a much larger magnetization reorientation in the ferromagnetic layer upon application of an electric field. In fact, by the electric field step of 0.32 MV m^{-1} the magnetization switches from an out-of-plane to an almost in-plane orientation as shown in Fig. 4(b). As expected, the magnetic anisotropy undergoes a dramatic change because of the compressive strain of 1.1% induced in the plane of $BaTiO_3$. A large fraction of this uniaxial strain is transferred to the magnetoelastically-coupled $[Co\backslash Ni]_4$ multilayer whose magnetization switches to in-plane via the inverse magnetostriction effect. Remarkably, the voltage that induces this magnetization switching is different from the voltage at which the ferroelectric reorients in Fig. 3(d). This mismatch strongly suggests that the ferroelectric reorientation observed in the X-ray microdiffraction experiment is a local effect taking place within and near the scanned area of 200 ×200 μm^2, rather than a macroscopic response of BTO-2. Such an early reorientation at 0.08 MV m^{-1} could be promoted by the presence of a *c*-domain in the vicinity of the scanned area at 0 MV m^{-1} (a few *c*-domains among predominantly in-plane domains were detected in BTO-2 by polarized light microscopy, Supplemental Material [22] section B). In contrast, other areas further away from *c*-domains would reorient at larger electric fields. Indeed, the coercive field of $BaTiO_3$ is around 0.1 MV m^{-1} [30], whereas its polarization saturation field is reported to be even larger, with values around 0.25 MV m^{-1} [7, 37]. Therefore, the electric field required for the *c*-domains to extend over the entire BTO-2 sample and, thus, to switch the magnetization of the strain-coupled $[Co\backslash Ni]_4$ multilayer, would be associated with the polarization saturation of the investigated $BaTiO_3$, which is likely to be in between 0.24 MV m^{-1} and 0.32 MV m^{-1}. In fact, in analogous $BaTiO_3$-based multiferroic composites, the strain-mediated magnetic switching takes place with applied electric fields above 0.24 MV m^{-1} [7, 10].

From this experimental result, we can calculate the converse magnetoelectric coupling coefficient (CMC) for BTO-2\ $[Co\backslash Ni]_4$, which is defined as a change in magnetization due to an external electric field, as $\propto_{CME} = \mu_0 \Delta M / \Delta E$. Since the magnetic remanence at 0.32 MV m^{-1} is 0.1, the induced change in magnetization ΔM can be estimated by multiplying the saturation magnetization of the $[Co\backslash Ni]_4$ stack ($M_S =$¿800 kA m^{-1}, measured on a reference film on silicon) by 0.9 (ΔM of a full 90º switching would be equal to the M_S value). ΔE is the required electric field to induce such a magnetization change. Hence, $\propto_{CME} =$¿ 2.8×10^{-6} s m^{-1} which is close to the highest CMCs reported so far [7,12,38], highlighting the outstanding magnetoelectric properties of this system (dislocation-free $BaTiO_3\backslash[Co\backslash Ni]_4$). Furthermore, it is worth emphasizing the difficulty of achieving a full voltage-controlled switching of the perpendicular magnetization to a

*maite.goiriena@ehu.eus

nearly in-plane orientation, which has been reported in only a very small number of works [10,39]. This switching is a key feature to a magnetoelectric memory device where in-plane and out-of-plane magnetic orientations would represent the digital 1 and 0 states.

Regarding the reversibility of the switching, it is believed that the BTO-2\[Co\Ni]$_4$ system would be suitable for applications with high repeatability, as demonstrated in an analogous $BaTiO_3$-based multiferroic composite [10]. This is in contrast with the case of BTO-1 whose fatigue behavior, and thus the reversibility of the BTO-1\[Co\Ni]$_4$ system, is constrained by the large density of dislocations and twin walls present in the initial state. Fatigue in the ferroelectric material certainly impacts the performance of the multiferroic heteresotructure. In the case of $BaTiO_3$, in addition to microstructural factors, electric-field-assisted migration of charged carriers, namely oxygen vacancies, can also play a major role. Fortunately, donor doping is known to significantly reduce this effect [40], and a recent work has found that within an electric field amplitude range, clustering of oxygen vacancies can be slowed, leading to almost fatigue-free $BaTiO_3$-based materials [41]. Despite these fatigue-reducing approaches and the optimum microstructural characteristics of BTO-2, the reversibility of the switching of BTO-2\[Co\Ni]$_4$, along with the nanostructuring of the ferromagnetic multilayer, ought to be the focus of future work.

In summary, a direct correlation between the coexistence of twin walls and dislocations in $BaTiO_3$ and its converse piezoelectric effect has been demonstrated by micro-strain mapping under a uniformly and systematically applied electric field. The ferroelectric domain motion is highly disrupted by the combination of a dense twinned structure and a large density of dislocations, whereas in a dislocation-free $BaTiO_3$ a full out-of-plane ferroelectric poling is observed, inducing the maximum achievable in-plane compressive strain of 1.1%. We have further studied the effect of these lattice defects on the voltage-controlled modulation of the PMA of [Co\Ni]$_4$ multilayer. Our results prove that in the absence of dislocations in $BaTiO_3$, the magnetization switches by 90° accompanied by a giant converse magnetoelectric coefficient $\propto_{CME}$ of 2.8×10^{-6} s m^{-1}. This finding highlights the major impact of the interaction between dislocations and twin walls in a ferroelectric substrate on the realization of highly energy-efficient magnetoelectric memory devices and, particularly, unveils the great promise held by $BaTiO_3$\[Co\Ni]$_4$ system.

This work was supported by the NSF Nanosystems Engineering Research Center for Translational Applications of the Nanoscale Multiferroic Systems (TANMS) under the Cooperative Agreement Award (EEC-1160504). The work made use of Advanced Light Source beamline 12.3.2 at Lawrence Berkeley National Laboratory, which is supported by the Director,

*maite.goiriena@ehu.eus

Office of Science, Office of Basic Energy Sciences, U.S. Department of Energy, under contract number DE-AC02-05CH11231. Part of this work was performed under the auspices of the U.S. Department of Energy by Lawrence Livermore National Laboratory under contract number DE-AC52-07NA27344. AC and FH magnetic characterization in this work were supported by the U.S. Department of Energy, Office of Science, Office of Basic Energy Sciences, Materials Sciences and Engineering Division under contract number DE-AC02-05CH11231 within the Nonequilibrium Magnetic Materials Program (MSMAG). Partial support was also provided by the National Science Foundation Center for Energy Efficient Electronics Science. M. Goiriena-Goikoetxea acknowledges the support of the Basque Government for the Postdoctoral Fellowship.

*maite.goiriena@ehu.eus

[1] M. S. Fashami, J. Atulasimha, and S. Bandyopadhyay, Magnetization dynamics, throughput and energy dissipation in a universal multiferroic nanomagnetic logic gate with fan-in and fan-out, Nanotech. **23**, 105201 (2012).

[2] S. Manipatruni, D. E. Nikonov, R. Ramesh, H. Li, and I. A. Young, Spin-orbit logic with magnetoelectric nodes: a scalable charge mediated nonvolatile spintronic logic, arXiv:1512.05428v2 (2017).

[3] M. Bibes, and A. Barthélémy, Towards magnetoelectric memory, Nat. Mater. **7**, 425 (2008).

[4] A. Brataas, A. D. Kent, and H. Ohno, Current-induced torques in magnetic materials, Nat. Mater. **11**, 372 (2012).

[5] L. Liu, C.-F. Pai, Y. Li, H. W. Tseng, D. C. Ralph, and R. A. Buhrman, Spin-torque switching with the giant spin Hall effect of tantalum, Science **336**, 555 (2012).

[6] J.-M. Hu, L.-Q. Chen, and C.W. Nan, Multiferroic heterostructures integrating ferroelectric and magnetic materials, Adv. Mater. **26**, 15 (2016).

[7] T. H. E. Lahtinen, K. J. A. Franke and S. van Dijken, Electric-field control of magnetic domain wall motion and local magnetization reversal, Sci. Rep. **2**, 258 (2012).

[8] T. H. E. Lahtinen, Y. Shirahata, L. Yao, K. J. A. Franke, G. Venkataiah, T. Taniyama and S. van Dijken, Alternating domains with uniaxial and biaxial magnetic anisotropy in epitaxial Fe films on $BaTiO_3$, Appl. Phys. Lett. **101**, 262405 (2012).

[9] R. V. Chopdekar, V. K. Malik, A. Fraile Rodríguez, L. Le Guyader, Y. Takamura, A. Scholl, D. Stender, C. W. Schneider, C. Bernhard, F. Nolting and L. J. Heyderman, Spatially resolved strain-imprinted magnetic states in an artificial multiferroic, Phys. Rev. B **86**, 014408 (2012).

[10] Y. Shirahata, R. Shiina, D. López González, K. J. A. Franke, E. Wada, M. Itoh, N. A. Pertsev, S. van Dijken and T. Taniyama, Electric-field switching of perpendicularly magnetized multilayers, NPG Asia Mater. **7**, e198 (2015).

[11] D. López González, Y. Shirahata, B. Van de Wiele, K. J. A. Franke, A. Casiraghi, T. Taniyama and S. van Dijken, Electric-field-driven domain wall dynamics in perpendicularly magnetized multilayers, AIP Adv. **7**, 035119 (2017).

[12] R. Lo Conte, J. Gorchon, A. Mougin, C. H. A. Lambert, A. El-Ghazaly, A. Scholl, S. Salahuddin and J. Bokor, Electrically controlled switching of the magnetization state in multiferroic $BaTiO_3$/CoFe submicrometer structures, Phys. Rev. Mater. **2**, 091402 (2018).

[13] E. I. Bondarenko, V. YU. Topolov and A. V. Turik, The role of 90° domain wall displacements in forming physical properties of perovskite ferroelectric ceramics, Ferroelectrics Lett. **13**, 13 (1991).

[14] Q. M. Zhang, H. Wang, N. Kim and L. E. Cross, Direct evaluation of domain-wall and intrinsic contributions to the dielectric and piezoelectric response and their temperature dependence on lead zirconate-titanate ceramics, J. Appl. Phys. **75**, 454 (1994).

[15] B. M. Park and S. J. Chung, Investigation of ferroelectric domains and structural twins in barium titanate crystal, Integr. Ferroelectr. **12**, 275 (1996).

[16] S. Jesse, B. J. Rodriguez, S. Choudhury, A. P. Baddorf, I. Vrejoiu, D. Hesse, M. Alexe, E. A. Eliseev, A. N. Morozovska, J. Zhang, L.-Q. Chen and S. V. Kalinin, Direct imaging of the spatial and energy distribution of nucleation centres in ferroelectric materials, Nat. Mat. **7**, 209 (2008).

[17] H. H. Wu, J. Wang, S. G. Cao and T. Y. Zhang, Effect of dislocation walls on the polarization switching of a ferroelectric single crystal, Appl. Phys. Lett. **102**, 232904 (2013).

*maite.goiriena@ehu.eus

[18] R. C. Bradt and G. S. Ansell, Dislocations and 90° domains in barium titanate, J. Appl. Phys. **38**, 5407 (1967).

[19] A. Kontsos and C. M. Landis, Computational modeling of domain wall interactions with dislocations in ferroelectric crystals, Int. J. Solids Struct. **46**, 1491 (2009).

[20] Z. Zhao, M. Jamali, N. D'Souza, D. Zhang, S. Bandyopadhyay, J. Atulasimha and J.-P. Wang, Giant voltage manipulation of MgO-based magnetic tunnel junctions via localized anisotropic strain: A potential pathway to ultra-energy-efficient memory technology, Appl. Phys. Lett. **109**, 092403 (2016).

[21] Q. Wang, X. Li, C.-Y. Liang, A. Barra, J. Domann, C. Lynch, A. Sepulveda and G. Carman, Strain-mediated 180° switching in CoFeB and Terfenol-D nanodots with perpendicular magnetic anisotropy, Appl. Phys. Lett. **110**, 102903 (2017).

[22] See Supplemental Material at [URL will be inserted by publisher] for information regarding the origin of the investigated $BaTiO_3$ crystals (section A), the polarized light microscopy images of BTO-1 and BTO-2 twin domain structures (section B), the analysis of the voltage-induced changes to the ferroelectric domain configuration in BTO-1 (section C) and the micro-strain maps of BTO-2 obtained by X-ray microdiffraction (section D).

[23] M. Kunz, N. Tamura, K. Chen, A. A. MacDowell, R. S. Celestre, M. M. Church, S. Fakra, E. E. Domning, J. M. Glossinger, J. L. Kirschman, G. Y. Morrison, D. W. Plate, B. V. Smith, T. Warwick, V. V. Yashchuk, H. A. Padmore and E. Ustundag, A dedicated superbend x-ray microdiffraction beamline for materials, geo-, and environmental sciences at the advanced light source, Rev. Sci. Instrum. **80**, 035108 (2009).

[24] R. Barabash, G. E. Ice, B. C. Larson, G. M. Pharr, K.-S. Chung and W. Yang, White microbeam diffraction from distorted crystals, Appl. Phys. Lett. **79**, 749 (2001).

[25] J. Nye, Some geometrical relations in dislocated crystals, Acta Metallurgica **1,** 153 (1953).

[26] E. Kroner, Continuum theory of dislocations and self-stresses, Ergebnisse der Angewandten Mathematik **5,** 1327 (1958).

[27] O. Eibl, P. Pongratz, P. Skalicky and H. Schmelz, Dislocations in $BaTiO_3$ ceramics, Phys. Stat. Sol. **108**, 495 (1988).

[28] J. Jiang, T. B. Britton and A. J. Wilkinson, Measurement of geometrically necessary dislocation density with high resolution electron backscatter diffraction: Effects of detector binning and step size, Ultramicroscopy **125**, 1 (2013).

[29] K. J. A. Franke, B. Van de Wiele, Y. Shirahata, S. J. Hämäläinen, T. Taniyama and S. van Dijken, Reversible electric-field-driven magnetic domain-wall motion, Phys. Rev. X **5,** 011010 (2015).

[30] H. H. Wieder, Ferroelectric hysteresis in barium titanate single crystals, J. Appl. Phys. **26**, 1479 (1955).

[31] M. He, M. Wang and Z. Zhang, Electric-field-induced domain intersection in $BaTiO_3$ single crystal, Jpn. J. Appl. Phys. **56**, 031501 (2017).

[32] M. T. Johnson, P. J. H. Bloemen, F. J. A. den Broeder and J. J. de Vries, Magnetic anisotropy in metallic multilayers, Rep. Prog. Phys. **59**, 1409 (1996).

[33] J. M. D. Coey, *Magnetism and Magnetic Materials* (Cambridge University Press, New York, 2010) p.388.

[34] R. C. O'Handley, *Modern Magnetic Materials: Principles and Applications* (Wiley-Interscience, New York, 2000) p.225.

[35] D. B. Gopman, C. L. Dennis, P. J. Chen, Y. L. Iunin, P. Finkel, M. Staruch and R. D. Shull, Strain-assisted magnetization reversal in Co/Ni multilayers with perpendicular magnetic anisotropy, Sci. Rep. **6**, 27774 (2016).

*maite.goiriena@ehu.eus

[36] N. Lei, S. Park, P. Lecoeur, D. Ravelosona and C. Chappert, Magnetization reversal assisted by the inverse piezoelectric effect in Co-Fe-B/ferroelectric multilayers, Phys. Rev. B. **84**, 012404 (2011).

[37] J.-H. Park, J. Park, K.-B. Lee, T.-Y. Koo, H. S. Youn, Y. D. Ko, J.-S. Chung, J. Y. Hwang, and S.-Y. Jeong, Local strain-induced 90° domain switching in a barium titanate single crystal, Appl. Phys. Lett. **91**, 012906 (2007).

[38] M. Staruch, D. B. Gopman, Y. L. Iunin, R. D. Shull, S. Fan Cheng, K. Bussmann and P. Finke, Reversible strain control of magnetic anisotropy in magnetoelectric heterostructures at room temperature, Sci. Rep. **6**, 37429 (2016).

[39] B. Peng, Z. Zhou, T. Nan, G. Dong, M. Feng, Q. Yang, X. Wang, S. Zhao, D. Xian, Z.-D. Jiang, W. Ren, Z.-G. Ye, N. X. Sun and M. Liu, Deterministic switching of perpendicular magnetic anisotropy by voltage control of spin reorientation transition in $(Co/Pt)_3/Pb(Mg_{1/3}Nb_{2/3})O_3$-$PbTiO_3$ multiferroic heterostructures, ACS Nano **11**, 4337 (2017).

[40] J. Chen, M. P. Harmer and D. M. Smyth, Compositional control of ferroelectric fatigue in perovskite ferroelectric ceramics and thin films, J. Appl. Phys. **76**, 5394 (1994).

[41] Z. Fan, J. Koruza, J. Rödel and X. Tan, An ideal amplitude window against electric fatigue in $BaTiO_3$-based lead-free piezoelectric materials, Acta Materialia **151,** 253 (2018).

*maite.goiriena@ehu.eus